Thermochemistry of Arylselanyl Radicals and the Pertinent Ions in Acetonitrile

ARTICLE *in* JOURNAL OF THE AMERICAN CHEMICAL SOCIETY · MARCH 2003

Impact Factor: 12.11 · DOI: 10.1021/ja0291787 · Source: PubMed

J|A|C|S
ARTICLES
Published on Web 02/01/2003

Thermochemistry of Arylselanyl Radicals and the Pertinent Ions in Acetonitrile

Allan Hjarbæk Holm,[†] Laura Yusta,[†] Peter Carlqvist,[‡] Tore Brinck,*[,‡] and Kim Daasbjerg*[,†]

Contribution from the Department of Chemistry, University of Aarhus, Langelandsgade 140, DK-8000 Aarhus C, Denmark, and Physical Chemistry, Royal Institute of Technology, SE-10044 Stockholm, Sweden

Received November 1, 2002; E-mail: kdaa@chem.au.dk

Abstract: Reduction and oxidation potentials of a series of parasubstituted phenylselanyl radicals, $XC_6H_4Se^{\bullet}$, have been measured using photomodulated voltammetry in acetonitrile. The thermodynamic significance of these data was substantiated through a study of the oxidation process of the pertinent selenolates in linear sweep voltammetry. Both the reduction and the oxidation potentials correlate linearly with the Hammett substituent coefficients σ and σ^+ leading in the latter case to slopes, ρ^+, of 2.5 and 3.8, respectively. Through comparison of these slopes with those published previously for the O- and S-centered analogues, it is revealed that the π-interaction becomes progressively smaller as the size of the radical center increases in the order O, S, and Se. Solvation energies of the pertinent selenolates and selanylium ions have been extracted from thermochemical cycles incorporating the measured electrode potentials for $XC_6H_4Se^{\bullet}$ as well as electron affinities and ionization potentials obtained from theoretical calculations at the B3LYP/6-31+G(d) level. The extracted data show the expected overall substituent dependency for both kinds of ions; that is, the absolute value of the solvation energy decreases as the charge becomes more delocalized. The data have also been compared with solvation energies computed using the polarizable continuum model (PCM). Interestingly, we find that, while the model seems to work well for selenolates, it underestimates the solvation of selanylium ions in acetonitrile by as much as 25 kcal mol^{-1}. These large deviations are ascribed to the fact that the PCM method does not take specific solvent effects into account as it treats the solvent as a continuum described solely by its dielectric constant. Gas-phase calculations show that the arylselanylium ions can coordinate covalently to one or two molecules of acetonitrile in strong Ritter-type adducts. When this strong interaction is included in the solvation energy calculations by means of a combined supermolecule and PCM approach, the experimental data are reproduced within a few kcal mol^{-1}. Although the energy difference of the singlet and triplet spin states of the arylselanylium ions is small for the gas-phase structures, the singlet cation is undoubtedly the dominating species in solution because the triplet cation lacks the ability to form covalent bonds.

Introduction

The important role of selenium compounds in both environmental and biological systems has long been recognized.[1,2] The synthetic applicability of selenium compounds is also well established and has been studied extensively over the past 15−20 years.[3] However, despite intensive research, very little is known about the redox properties of selenium compounds. A few papers have been devoted to electrochemical investigations of diselenides,[4,5] but no reports have appeared so far on the reactive free radical and ionic species.

In this paper, we wish to present our results concerning the reduction and oxidation of a series of parasubstituted phenylselanyl radicals (Scheme 1) in acetonitrile by employing the photomodulated voltammetry (PMV) technique.[6] Because the standard potentials of the substituted phenylselanyl radicals can be determined by linear sweep voltammetry (LSV) as well, it will be possible to verify the reliability of the PMV measurements. The extent of interaction between the π-system of the aromatic ring and the orbitals of the adjacent atoms may be evaluated through a comparison of slopes obtained in Hammett plots of the potentials with those published previously for the O- and S-centered analogues.

Another point addressed by the present study is the solvation energies of the ions formed upon reduction and oxidation of the selanyl radicals. These solvation energies are extracted from

[†] University of Aarhus.
[‡] Royal Institute of Technology.

(1) Shamberger, R. J. *Biochemistry of Selenium*; Plenum: New York, 1983.
(2) Soda, K.; Tanaka, H.; Esaki, N. In *The Chemistry of Organic Selenium and Tellurium Compounds*; Patai, S., Ed.; John Wiley: New York, 1987; Vol. 2, Chapter 7.
(3) *Organoselenium Chemistry: Modern Developments in Organic Synthesis*, *Top. Curr. Chem.*; Wirth, T., Ed.; Springer-Verlag: Berlin, Heidelberg, New York, 2000; Vol. 208 and references therein.
(4) Giles, G. I.; Tasker, K. M.; Johnson, R. J. K.; Jacob, C.; Peers, C.; Green, K. N. *Chem. Commun.* **2001**, 2490.
(5) Latypova, V. Z.; Chichirov, A. A.; Zhuikov, V. V.; Yakovleva, O. G.; Vinokurova, R. I.; Ustyugova, I. A.; Kargin, Y. M. *Zh. Obshch. Khim.* **1989**, *59*, 1344.
(6) Wayner, D. D. M.; Griller, D. *J. Am. Chem. Soc.* **1985**, *107*, 7764.

10.1021/ja0291787 CCC: $25.00

Scheme 1

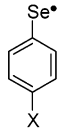

X = $N(CH_3)_2$, OCH_3, CH_3, F, H, Cl, Br, CN, or NO_2

thermochemical cycles incorporating the measured potentials and electron affinities and ionization potentials obtained from theoretical calculations. This provides the possibility of testing one of the most successful solvation models, the polarizable continuum model (PCM),[7−10] on a series of relatively large ions. So far, its success has mainly relied on the study of neutral molecules and relatively small and localized ions.[7−10] In recent studies on carbanions,[11] thiophenoxides,[12] and arylsulfenium ions,[12] we have shown that, while the model can be applied successfully for the anions, it underestimates the absolute value of the solvation energy of the cations in acetonitrile. On the basis of supermolecule calculations, this was attributed to a strong specific solvation in terms of a Ritter-type adduct formed between the sulfur atom of the sulfenylium ion and one molecule of acetonitrile.[12] For the selanylium ions, the possibility of having similar interactions seems plausible, although the larger size of Se as compared to S might lead to other effects as well. Also it will be considered for both gas phase and solution if the spin state of arylselanylium ions is a triplet or a singlet by calculating the energy difference using high levels of theory.

Experimental Section

Materials. Bis(4-chlorophenyl) and diphenyl diselenide were obtained commercially from Aldrich and Lancaster, respectively, and used as received. Bis(4-bromophenyl),[13] bis(4-cyanophenyl),[14] bis(4-dimethylamino),[15] bis(4-fluorophenyl),[13] bis(4-methoxyphenyl),[13] bis(4-methylphenyl),[13] and bis(4-nitrophenyl) diselenide[14] were prepared according to the references cited. The crude products contained varying amounts (2−25%) of the corresponding monoselenide, which was removed in a reductive purification procedure.[16] Acetonitrile was obtained from Lab-Scan and dried through a column of activated alumina. The supporting electrolyte, tetrabutylammonium tetrafluoroborate (Bu_4NBF_4), was prepared and purified by standard procedures.

Apparatus. The instrumental setup used in the photomodulated voltammetry technique has been described in detail recently.[11,17,18] It consisted of a 200 W Hg−Xe lamp (Photon Technology International) for generating radicals photolytically, a water filter, a chopper (651, EG&G Instruments), a lock-in amplifier (SR810 DSP, Stanford Research Systems), and a home-built electrochemical flow-cell for detecting the radicals. A net made of carbon fibers (transparency of at least 50%) was used as working electrode. A small platinum rod positioned in the outlet of the electrochemical cell served as counter electrode. The reference electrode was a Flex-Ref electrode purchased from World Precision Instruments. In the linear sweep experiments, a $\phi = 1$ mm glassy carbon (Sigradur G, HTW) disk was employed as working electrode. The electrode surface was carefully polished before each experiment with a 0.25 μm diamond suspension and rinsed in ethanol. The counter electrode was a platinum coil melted into glass, while a Ag wire in 0.1 M Bu_4NBF_4/acetonitrile separated from the solution by a sintered glass tube served as quasi-reference electrode. The ohmic drop in both the LSV and the PMV experiments was compensated with a positive feedback system incorporated in the homemade potentiostat.

Procedure. The method employed for generating the arylselanyl radicals in the PMV experiments consisted of photolyzing the appropriate diselenide as shown in eq 1.

$$(XC_6H_4Se\text{-})_2 \xrightarrow{h\nu} 2XC_6H_4Se^{\bullet} \quad (1)$$

The concentration of diselenide was typically 10 mM in a deaerated solution of 0.1 M Bu_4NBF_4/acetonitrile. Samples were allowed to flow through the cell at a rate of 2−3 mL min^{-1} to prevent depletion of substrate and product accumulation. An output of 100 W from the lamp was sufficient for photolyzing the different diselenides. Under these conditions, the temperature near the electrode surface did not exceed 26 °C within an experiment as measured by a temperature sensitive probe. The chopping frequency employed was 134 Hz. The sweep rate was usually 0.1 V s^{-1}. The voltammograms were corrected for the background current recorded in the absence of substrate. All half-wave potentials were referenced to SCE by measuring them relative to the standard potential of the ferrocenium/ferrocene redox couple (= 0.41 V versus SCE).[19]

The precursors used in the LSV studies, the substituted selenolates, were generated in 1−2 mM concentration by a preparative two-electron reduction of the pertinent diselenides in 0.1 M Bu_4NBF_4/acetonitrile according to eq 2.

$$(XC_6H_4Se\text{-})_2 + 2e \rightarrow 2XC_6H_4Se^{-} \quad (2)$$

The sweep rates employed were in the range 0.2−20 V s^{-1}. All potentials were measured relative to the standard potential of anthracene (= −1.955 V versus SCE in 0.1 M Bu_4NBF_4/acetonitrile) and referenced to SCE. Adsorption problems could be overcome by pretreating the electrodes using multiscans.[20] We did note, however, that the peak potentials could vary by as much as 30 mV from one series of experiments to another when employing different glassy carbon electrodes. All solutions were carefully deaerated with argon before use.

Digital simulations were performed using the DigiSim version 3.03 software (Bioanalytical Systems, Inc.).[21] In all simulations, the transfer coefficient was set equal to 0.5. The diffusion coefficient was measured for a number of selenolates and found to be $(1.0 \pm 0.1) \times 10^{-5}$ cm^{-2} s^{-1}.[22]

Solvation Energies. The formal relationships used for extracting the two differential solvation energies, $\Delta\Delta G^{\circ}_{sol}(+\bullet)_{exp}$ and $\Delta\Delta G^{\circ}_{sol}(-\bullet)_{exp}$, from the experimentally obtained electrode potentials are shown in eqs 3 and 4.[23,24]

$$\Delta\Delta G^{\circ}_{sol}(+\bullet)_{exp} \equiv \Delta G^{\circ}_{sol}(+)_{exp} - \Delta G^{\circ}_{sol}(\bullet)_{exp} = -IP + FE^{\circ}_{XC_6H_4Se^{+}/XC_6H_4Se^{\bullet}} + C \quad (3)$$

(7) Tomasi, J.; Persico, M. *Chem. Rev.* **1994**, *94*, 2027 and references therein.
(8) Cossi, M.; Barone, V.; Cammi, R.; Tomasi, J. *Chem. Phys. Lett.* **1996**, *255*, 327.
(9) Menucci, B.; Tomasi, J. *J. Chem. Phys.* **1997**, *106*, 5151.
(10) Barone, V.; Cossi, M.; Tomasi, J. *J. Chem. Phys.* **1997**, *107*, 3210.
(11) Brinck, T.; Larsen, A. G.; Madsen, K. M.; Daasbjerg, K. *J. Phys. Chem. B* **2000**, *104*, 9887.
(12) Brinck, T.; Carlqvist, P.; Holm, A. H.; Daasbjerg, K. *J. Phys. Chem. A* **2002**, *106*, 8827.
(13) Schmid, G. H.; Garratt, D. G. *J. Org. Chem.* **1983**, *48*, 4169.
(14) Syper, L.; Mlochowski, J. *Tetrahedron* **1988**, *44*, 6119.
(15) Bauer, H. *Chem. Ber.* **1913**, *46*, 92.
(16) Uneyama, K.; Maeda, K.; Tokunaga, Y. *J. Org. Chem.* **1995**, *60*, 370.
(17) Larsen, A. G.; Holm, A. H.; Roberson, M.; Daasbjerg, K. *J. Am. Chem. Soc.* **2001**, *123*, 1723.
(18) Lund, T.; Wayner, D. D. M.; Jonsson, M.; Larsen, A. G.; Daasbjerg, K. *J. Am. Chem. Soc.* **2001**, *123*, 12590.
(19) Daasbjerg, K.; Pedersen, S. U.; Lund, H. In *General Aspects of the Chemistry of Radicals*; Alfassi, Z. B., Ed.; John Wiley: Chichester, 1999; Chapter 12, p 410.
(20) Christensen, T. B.; Daasbjerg, K. *Acta Chem. Scand.* **1997**, *51*, 307.
(21) Rudolph, M.; Feldberg, S. W. *DigiSim version 3.03*; Bioanalytical Systems, Inc.
(22) Occhialini, D.; Pedersen, S. U.; Daasbjerg, K. *J. Electroanal. Chem.* **1994**, *369*, 39.
(23) Matsen, F. A. *J. Chem. Phys.* **1956**, *24*, 602.
(24) Peover, M. E. *Trans. Faraday Soc.* **1962**, *58*, 1656.

$$\Delta\Delta G^\circ_{sol}(-\bullet)_{exp} \equiv \Delta G^\circ_{sol}(-)_{exp} - \Delta G^\circ_{sol}(\bullet)_{exp} = EA - FE^\circ_{XC_6H_4Se^\bullet/XC_6H_4Se^-} - C \quad (4)$$

The parameters $\Delta G^\circ_{sol}(+)$, $\Delta G^\circ_{sol}(-)$, and $\Delta G^\circ_{sol}(\bullet)$ denote the solvation energies of the selenium-centered ions and radicals, while IP and EA are the ionization potential and electron affinity of the arylselanyl radicals, respectively. The two latter parameters are calculated using the B3LYP/6-31+G(d) approach as described below. For the constant C, a number of 109.3 kcal mol^{-1} is used, which originates from the value of the absolute potential of the standard calomel electrode (= −4.74 V).[25,26]

In this context, it is also interesting to have a closer look at the difference of $\Delta\Delta G^\circ_{sol}(+\bullet)_{exp}$ and $\Delta\Delta G^\circ_{sol}(-\bullet)$ expressed as the parameter $\Delta\Delta G^\circ_{sol}(\pm)_{exp}$ in eq 5.

$$\Delta\Delta G^\circ_{sol}(\pm)_{exp} \equiv \Delta\Delta G^\circ_{sol}(+\bullet)_{exp} - \Delta\Delta G^\circ_{sol}(-\bullet)_{exp} = -(IP + EA) + F(E^\circ_{XC_6H_4Se^+/XC_6H_4Se^\bullet} + E^\circ_{XC_6H_4Se^\bullet/XC_6H_4Se^-}) + 2C \quad (5)$$

As the $\Delta\Delta G^\circ_{sol}(\pm)_{exp}$ parameter is independent of the radical species, it should provide a good description of the solvation features of the ions.

Theoretical Approach. Optimized geometries and harmonic frequencies for all molecules have been computed at the B3LYP/6-31+G(d) level of theory. The B3LYP functional[27] is a modification of the three-parameter exchange-correlation functional of Becke.[28] In addition to the gradient-corrected exchange and correlation functionals of Becke[29] and Lee et al.,[30] respectively, it includes a part of the Hartree−Fock exchange-energy. Single point energies were computed at the B3LYP/6-31+G(3df,2p) level of theory using the B3LYP/6-31+G(d) optimized geometries. However, it was found that these calculations gave results only marginally different from the B3LYP/6-31+G(d) energies, and therefore we will only report the latter set of data in this article. Zero point, enthalpy, and free energy corrections to the electronic energies have been calculated on the basis of the unscaled B3LYP/6-31+G(d) frequencies.

In this study, we have also calculated geometries and energies of some molecular complexes at the MP2/6-31+G(d) level of theory. The MP2 method is generally less reliable than the B3LYP method for studying processes that involve breaking or formation of covalent bonds. On the other hand, MP2 is more accurate than B3LYP for nonbonded interactions, because it provides a proper description of the dispersion component of the interaction energy.

Solvation energies $\Delta G^\circ_{sol}(+)_{PCM}$, $\Delta G^\circ_{sol}(-)_{PCM}$, and $\Delta G^\circ_{sol}(\bullet)_{PCM}$ of the Se-centered ions and radicals have been calculated at the B3LYP/6-31+G(d) level using the recent implementation of the polarizable continuum model (PCM)[8] in Gaussian 98.[31] The solute cavities in these calculations were made up of overlapping spheres centered at the atomic nuclei. The radii of the spheres were taken as the van der Waals radii[32] implemented in Gaussian 98 and scaled by a constant of 1.2 for all atoms except acidic hydrogens.[31] The solvent parameters, including the dielectric constant, were the same as those given for acetonitrile in the program.

To investigate the importance of specific solute−solvent interactions, we have included calculations of solvation energies for the cations using a supermolecule approach. In this approach, we combine an explicit treatment of one or two solvent molecules with the use of the PCM method for estimating the remaining part of the solvation energy. We have previously used similar methods successfully to study the catalytic mechanism for hydrolysis of the methyl phosphate anion in aqueous solution[33] and to study the solvation of arylsulfenium ions and thiophenoxides in acetonitrile.[12] The expression for the solvation energy of arylselanylium ions coordinated to one explicit acetonitrile molecule, $\Delta G^\circ_{sol}(+)_{sup}$, is given in eq 6.

$$\Delta G^\circ_{sol}(+)_{sup} = \Delta G^\circ_{1\rightarrow g}(CH_3CN) + \Delta G^\circ_g(CH_3CN + XC_6H_4Se^+ \rightarrow XC_6H_4Se^+\text{-}NCCH_3) + \Delta G^\circ_{sol}(XC_6H_4Se^+\text{-}NCCH_3)_{PCM} \quad (6)$$

In this expression, $\Delta G^\circ_{1\rightarrow g}(CH_3CN)$ is the free energy required to transfer one molecule of acetonitrile from the liquid phase to the gas phase at a concentration of 1 mol dm^{-3}. The value of $\Delta G^\circ_{1\rightarrow g}(CH_3CN)$ is estimated to be 3.91 kcal mol^{-1} from the vapor pressure (25 mmHg)[34] of acetonitrile at 298 K. The term $\Delta G^\circ_g(CH_3CN + XC_6H_4Se^+ \rightarrow XC_6H_4Se^+\text{-}NCCH_3)$ corresponds to the free energy of binding one molecule of acetonitrile to $XC_6H_4Se^+$ in the gas phase at a concentration of 1 mol dm^{-3}, and $\Delta G^\circ_{sol}(XC_6H_4Se^+\text{-}NCCH_3)_{PCM}$ is the PCM computed solvation energy of $XC_6H_4Se^+\text{-}NCCH_3$ at the same concentration. Formally, eq 6 is derived from a thermochemical cycle where one acetonitrile molecule is transferred to the gas phase, binds to $XC_6H_4Se^+$ to form the adduct $XC_6H_4Se^+\text{-}NCCH_3$, which then is transferred to the acetonitrile solution. The corresponding expression for the coordination of two acetonitrile molecules to $XC_6H_4Se^+$ is shown in eq 7.

$$\Delta G^\circ_{sol}(+)_{sup2} = 2\Delta G^\circ_{1\rightarrow g}(CH_3CN) + \Delta G^\circ_g[2CH_3CN + XC_6H_4Se^+ \rightarrow XC_6H_4Se^+\text{-}(NCCH_3)_2] + \Delta G^\circ_{sol}[XC_6H_4Se^+\text{-}(NCCH_3)_2]_{PCM} \quad (7)$$

To obtain solvation energies that are directly comparable with the experimentally obtained $\Delta\Delta G^\circ_{sol}(+\bullet)_{exp}$ values, we have combined $\Delta G^\circ_{sol}(+)_{sup}$ and $\Delta G^\circ_{sol}(+)_{sup2}$ with $\Delta G^\circ_{sol}(\bullet)_{PCM}$ computed using the PCM method according to eqs 8 and 9.

$$\Delta\Delta G^\circ_{sol}(+\bullet)_{sup} = \Delta G^\circ_{sol}(+)_{sup} - \Delta G^\circ_{sol}(\bullet)_{PCM} \quad (8)$$

$$\Delta\Delta G^\circ_{sol}(+\bullet)_{sup2} = \Delta G^\circ_{sol}(+)_{sup2} - \Delta G^\circ_{sol}(\bullet)_{PCM} \quad (9)$$

It should be noted that eq 8 differs from the expression used to calculate $\Delta\Delta G^\circ_{sol}(+\bullet)_{sup}$ in our previous study on solvation of arylsulfenium cations,[12] where a supermolecule approach also was used for the pertinent radical species. However, in this study, we choose to use a pure PCM calculation, because supermolecule approaches can be less accurate when the solute−solvent interaction in the first solvation shell is very weak.

Results and Discussion

Half-Wave Potentials. a) PMV. Figure 1 shows the photomodulated voltammogram of $C_6H_5Se^\bullet$ generated from photolysis of diphenyl diselenide (see eq 1). The two characteristic steady-state waves pertain to the generalized electrode processes shown in eqs 10 and 11.

(25) Reiss, H.; Heller, A. *J. Phys. Chem.* **1985**, *89*, 4207.
(26) Lim, C.; Bashford, D.; Karplus, M. *J. Phys. Chem.* **1991**, *95*, 5610.
(27) Stephens, P. J.; Devlin, F. J.; Chablovski, C. F.; Frisch, M. J. *J. Phys. Chem.* **1994**, *98*, 11623.
(28) Becke, A. D. *J. Chem. Phys.* **1993**, *98*, 5648.
(29) Becke, A. D. *J. Chem. Phys.* **1988**, *96*, 2155.
(30) Lee, C.; Yang, W.; Parr, R. G. *Phys. Rev. B* **1988**, *33*, 3098.
(31) Frisch, M. J.; Trucks, G. W.; Schlegel, H. B.; Scuseria, G. E.; Robb, M. A.; Cheeseman, J. R.; Zakrzewski, V. G.; Montgomery, J. A., Jr.; Stratmann, R. E.; Burant, J. C.; Dapprich, S.; Millam, J. M.; Daniels, A. D.; Kudin, K. N.; Strain, M. C.; Farkas, C. O.; Tomasi, J.; Barone, V.; Cossi, M.; Cammi, R.; Mennucci, B.; Pomelli, C.; Adamo, C.; Clifford, S.; Ochterski, J.; Petersson, G. A.; Ayala, P. Y.; Cui, Q.; Morokuma, K.; Malick, D. K.; Rabuck, A. D.; Raghavachari, K.; Foresman, J. B.; Cioslowski, J.; Ortiz, J. V.; Baboul, A. G.; Stefanov, B. B.; Liu, G.; Liashenko, A.; Piskorz, P.; Komaromi, I.; Gomperts, R.; Martin, R. L.; Fox, D. J.; Keith, T.; Al-Laham, M. A.; Peng, C. Y.; Nanayakkara, A.; Gonzalez, C.; Challacombe, M.; Gill, P. M. W.; Johnson, B. G.; Chen, W.; Wong, M. W.; Andres, J. L.; Head-Gordon, M.; Replogle, E. S.; Pople, J. A. *Gaussian 98*, revision A.7; Gaussian, Inc.: Pittsburgh, PA, 1998.
(32) Bondi, A. *J. Phys. Chem.* **1964**, *68*, 441.
(33) Hu, C.-H.; Brinck, T. *J. Phys. Chem. A* **1999**, *103*, 5379.
(34) Weissberger, A.; Proskauer, E. S.; Riddik, J. A.; Toops, E. E. *Organic Solvents*, 2nd ed.; Interscience Publishers: New York, 1955; p 224.

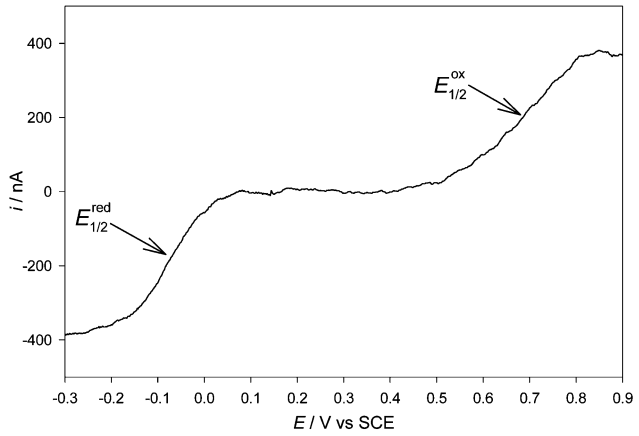

Figure 1. Background-corrected photomodulated voltammogram of the phenylselanyl radical, $C_6H_5Se^{\bullet}$, generated by photolysis of 10 mM diphenyl diselenide at a carbon fiber net in a 0.1 M Bu_4NBF_4/acetonitrile solution. Sweep rate = 0.1 V s^{-1}.

$$XC_6H_4Se^+ + e \rightleftharpoons XC_6H_4Se^{\bullet} \quad (10)$$

$$XC_6H_4Se^{\bullet} + e \rightleftharpoons XC_6H_4Se^- \quad (11)$$

In Table 1, the half-wave potentials, $E^{ox}_{1/2}$ and $E^{red}_{1/2}$, obtained for the series of parasubstituted phenylselanyl radicals are collected along with the characteristic width of the waves, $|E_{3/4} - E_{1/4}|$. For a nernstian process unaffected by preceding or follow-up chemistry, $|E_{3/4} - E_{1/4}|$ should be equal to 56.4 mV.[35] The large values of 85−155 mV observed experimentally for the present systems would usually indicate that the charge-transfer kinetics at the electrode surface are relatively slow.[36] The consequence of such a quasi-reversible behavior would be that $E^{ox}_{1/2}$ and $E^{red}_{1/2}$ are shifted in the positive and negative direction, respectively, relative to the pertinent standard potentials $E^{\circ}_{XC_6H_4Se^+/XC_6H_4Se^{\bullet}}$ and $E^{\circ}_{XC_6H_4Se^{\bullet}/XC_6H_4Se^-}$. However, there could also be an effect on the position of the waves from fast homogeneous reactions involving $XC_6H_4Se^+$ and $XC_6H_4Se^{\bullet}$.[36] While $XC_6H_4Se^-$ has a high stability in aprotic solvents, $XC_6H_4Se^{\bullet}$ is expected to dimerize in a fast process, and $XC_6H_4Se^+$ would as a strong electrophile react with any nucleophile present in the solution, be it residual water or the solvent itself. Consequently, the values of $E^{ox}_{1/2}$ and $E^{red}_{1/2}$ cannot a priori be set equal to the standard potentials $E^{\circ}_{XC_6H_4Se^+/XC_6H_4Se^{\bullet}}$ and $E^{\circ}_{XC_6H_4Se^{\bullet}/XC_6H_4Se^-}$. In principle, simulation of the voltammetric curves might provide some useful information, but the combined effect of the homogeneous and heterogeneous kinetics is a complicating factor that makes a quantitative estimation of the difference between $E_{1/2}$ and E° difficult.[36] Things are even further complicated by the fact that the distribution of radicals will be nonhomogeneous due to the variable light intensity along the absorption path and, especially, by the shielding effect of the net used as working electrode.

b) LSV. Because of the uncertainties present in the interpretation of the photomodulated voltammetry experiments, we pursued another approach for judging the thermodynamic significance of the measured half-wave potentials. This approach consisted of studying the oxidation of the selenolates, that is, the reverse of eq 11, taking advantage of the fact that stable solutions of selenolates could easily be generated in acetonitrile by carrying out a preparative reduction of the corresponding diselenides in a two-electron process (see eq 2). Note that the same methodology would not be applicable in the case of selanylium ions due to their high reactivity on this time scale.

In Figure 2, linear sweep voltammograms are collected for all substituted phenylselenolates with the characteristic irreversible one-electron oxidation wave appearing in the range of −0.41 V versus SCE for X = $N(CH_3)_2$ to 0.09 V versus SCE for X = CN at a sweep rate of 1 V s^{-1}. The plot of the oxidation peak potential, E^{ox}_p, versus the logarithm of the sweep rate, log ν, depicted in Figure 3 in the case of X = H shows that there exists a linear relationship in the sweep rate range of 0.2−2 V s^{-1} followed by distinct deviations when larger values of ν are applied.

The slope of the linear section is close to 20 mV $decade^{-1}$, which is consistent with a rapid heterogeneous electron transfer, eq 12, followed by a fast dimerization reaction, eq 13, formally described as an E_rC_2 mechanism.[35]

$$XC_6H_4Se^- - e \rightleftharpoons XC_6H_4Se^{\bullet} \quad (12)$$

$$2XC_6H_4Se^{\bullet} \xrightarrow{k_d} (XC_6H_4Se\text{-})_2 \quad (13)$$

In this region, the kinetic control is fully by the follow-up reaction, and E^{ox}_p is related to $E^{\circ}_{XC_6H_4Se^{\bullet}/XC_6H_4Se^-}$ through eq 14.[37,38]

$$E^{ox}_p = E^{\circ}_{XC_6H_4Se^{\bullet}/XC_6H_4Se^-} + 0.902\frac{RT}{F} - \frac{RT}{3F}\ln\left(\frac{2k_dC^o}{\nu}\frac{2RT}{3F}\right) \quad (14)$$

In the above expression, $2k_d$ is the dimerization rate constant, and C^o is the bulk concentration of the arylselenolate. If a reasonable estimate of $2k_d$ can be provided, it is possible to determine $E^{\circ}_{XC_6H_4Se^{\bullet}/XC_6H_4Se^-}$. In this study, we assume that 10^9 M^{-1} s^{-1} < $2k_d$ < 4×10^{10} M^{-1} s^{-1} in line with the assessment made by Andrieux et al. on arylthiyl radicals.[39] The upper limit is simply set as the diffusion-controlled rate constant in acetonitrile. The lower limit is estimated on the basis of fast cyclic voltammetry; even at sweep rates of 10 kV s^{-1} using a 0.6 mM selenolate concentration it was impossible to outrun the dimerization reaction and detect the selanyl radical in terms of a reduction wave on the reverse scan. Thus, a midpoint value (on a logarithmic scale) of $2k_d = 6.3 \times 10^9$ M^{-1} s^{-1} is used in the calculations of $E^{\circ}_{XC_6H_4Se^{\bullet}/XC_6H_4Se^-}$, resulting in an uncertainty on its determination of ±0.03 V corresponding to ±0.7 kcal mol^{-1} when expressed in free energy terms. The $E^{\circ}_{XC_6H_4Se^{\bullet}/XC_6H_4Se^-}$ values are collected in Table 1.

The curved section of the E^{ox}_p versus log ν plot in Figure 3 observed at sweep rates above 2 V s^{-1} is consistent with a gradual shift in the kinetic control from the follow-up reaction to the initial electron-transfer step.[40−42] Under such conditions of mixed kinetic control, it will be possible to estimate the het-

(35) Bard, A. J.; Faulkner, L. R. *Electrochemical Methods, Fundamentals and Applications*; John Wiley: New York, 1980.
(36) Nagaoka, T.; Griller, D.; Wayner, D. D. M. *J. Phys. Chem.* **1991**, *95*, 6264.
(37) Savéant, J.-M.; Vianello, E. *Electrochim. Acta* **1967**, *12*, 1545.
(38) Andrieux, C. P.; Nadjo, L.; Savéant, J.-M. *J. Electroanal. Chem.* **1973**, *42*, 223.
(39) Andrieux, C. P.; Hapiot, P.; Pinson, J.; Savéant, J.-M. *J. Am. Chem. Soc.* **1993**, *115*, 7783.
(40) Nadjo, L.; Savéant, J.-M. *J. Electroanal. Chem.* **1973**, *48*, 113.
(41) Savéant, J.-M.; Vianello, E. *C. R. Hebd. Seances Acad. Sci.* **1963**, *256*, 2597.
(42) Andrieux, C. P.; Savéant, J.-M. In *Investigations of Rates and Mechanisms of Reactions, Techniques of Chemistry*; Bernasconi, C. F., Ed.; Wiley: New York, 1986; Vol. VI/4E, Part 2, pp 305−390.

Table 1. Half-Wave Potentials $E^{ox}_{1/2}$ and $E^{red}_{1/2}$ and Peak Widths $|E_{3/4} - E_{1/4}|$ Measured for $XC_6H_4Se^{\bullet}$ by Means of Photomodulated Voltammetry at a Carbon Fiber Net along with $E^{\circ}_{XC_6H_4Se^{\bullet}/XC_6H_4Se^-}$ Values Obtained from Linear Sweep Experiments at a Glassy Carbon Electrode in 0.1 M Bu_4NBF_4/Acetonitrile; Computed Singlet and Triplet Ionization Potentials, IP(S) and IP(T), and Electron Affinities, EA, for $XC_6H_4Se^{\bullet}$

X	$E^{ox}_{1/2}$ [a,c]	$\|E_{3/4} - E_{1/4}\|$ [b]	$E^{red}_{1/2}$ [a,c]	$\|E_{3/4} - E_{1/4}\|$ [b]	$E^{\circ}_{XC_6H_4Se^{\bullet}/XC_6H_4Se^-}$ [a,d]	IP(S)[e]	IP(T)[e]	EA[e]
$N(CH_3)_2$	0.27	88	−0.28	117	−0.34	6.88	7.17	1.92
OCH_3	0.61	144	−0.15	114	−0.14	7.57	7.75	2.06
CH_3	0.62	155	−0.13	116	−0.10	8.16	7.97	2.16
F	0.70	147	−0.06	128	−0.03	8.34	8.29	2.36
H	0.70	148	−0.06	131	−0.04	8.33	8.19	2.25
Cl	0.73	130	−0.05	110	0.02	8.27	8.24	2.47
Br	0.74	124	−0.02	111	−0.01	8.20	8.18	2.50
CN	0.82	137	0.05	99	0.17	8.78	8.58	2.93
NO_2	*f*	*f*	0.09	85	0.16	9.03	8.76	3.20

[a] V versus SCE. [b] In mV. [c] Determined at a sweep rate of 0.1 V s^{-1} with an uncertainty of ±30 mV; average of at least four determinations. [d] Uncertainty is ±30 mV. [e] In eV, calculated at the B3LYP/6-31+G(d) level using the Gaussian 98 suite of programs. [f] No reproducible oxidation wave was observable in this case.

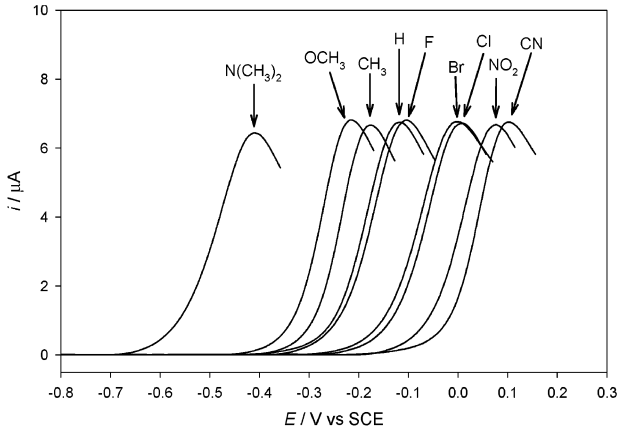

Figure 2. Linear sweep voltammograms recorded for the oxidation of 1 mM arylselenolate, $XC_6H_4Se^-$, at a glassy carbon electrode in a 0.1 M Bu_4NBF_4/acetonitrile solution. Sweep rate = 1 V s^{-1}.

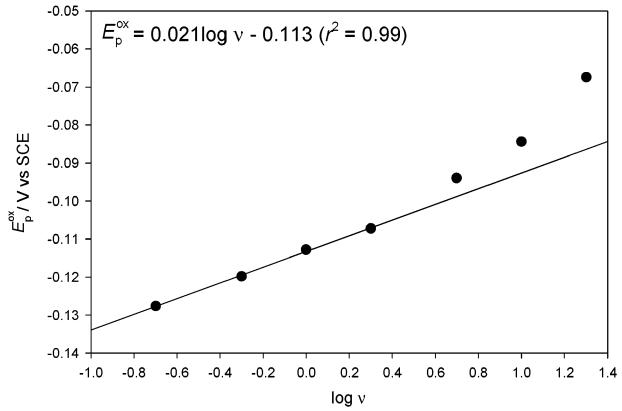

Figure 3. Plot of E^{ox}_p versus log ν for the oxidation of 1 mM phenylselenolate. Sweep rates of 0.2−20 V s^{-1} are applied, but only the four points pertaining to the 0.2−2 V s^{-1} range are included in the linear regression.

erogeneous rate constant, k^o, through simulation of the experimental voltammograms using the DigiSim software.[21] In the simulations, we choose to keep the $E^{\circ}_{XC_6H_4Se^{\bullet}/XC_6H_4Se^-}$ values determined from the linear section of the E^{ox}_p versus log ν plot fixed as this seemed to give the most consistent results. Still, it should be emphasized that the variation in $E^{\circ}_{XC_6H_4Se^{\bullet}/XC_6H_4Se^-}$ never exceeded 20 mV even if it was treated as a variable in the program.

The extracted values of k^o are all close to 0.1 cm s^{-1}, independent of the substituent, and quite similar to those obtained previously for the thiophenoxides.[39] With the finding of rather large values for k^o, it seems precluded that the photomodulated voltammograms recorded at $\nu = 0.1$ V s^{-1} should be influenced by slow charge-transfer kinetics. In other words, the relatively broad reduction waves with $|E_{3/4} - E_{1/4}|$ values of 85−131 mV cannot be related specifically to the chemical system inasmuch as the experimental limitations of the PMV technique discussed above. This conclusion is reinforced by the fact that exactly the same tendency has been observed in our previous studies on arylthiyl[17] and α-hydroxy alkyl radicals.[18] Moreover, there is no correlation between the k^o and $|E_{3/4} - E_{1/4}|$ values.

In view of the above-mentioned limitations of the PMV technique, the question is how reliable the measured half-wave potentials can be considered from a thermodynamic point of view? A comparison of the two sets of $E^{red}_{1/2}$ and $E^{\circ}_{XC_6H_4Se^{\bullet}/XC_6H_4Se^-}$ data in Table 1 reveals that the agreement is actually quite good with an absolute mean deviation of 50 mV. These observations are consistent with those in our previous studies on arylthiyl[17] and α-hydroxy alkyl radicals.[18] There is no relationship between $|E_{3/4} - E_{1/4}|$ and the differences observed in the potentials. For instance, the reduction wave pertaining to X = CN is relatively sharp with $|E_{3/4} - E_{1/4}| = 99$ mV, but still $E^{red}_{1/2}$ is smaller than $E^{\circ}_{XC_6H_4Se^{\bullet}/XC_6H_4Se^-}$ by 120 mV. In contrast to this stands the agreement within 20 mV between $E^{red}_{1/2}$ and $E^{\circ}_{XC_6H_4Se^{\bullet}/XC_6H_4Se^-}$ for X = H, even if $|E_{3/4} - E_{1/4}|$ is as large as 131 mV. In view of the overall good agreement between $E^{red}_{1/2}$ and $E^{\circ}_{XC_6H_4Se^{\bullet}/XC_6H_4Se^-}$ and the fact that all other photomodulated waves have similar widths ranging between 88 and 155 mV, we conclude that the measured $E^{ox}_{1/2}$ and $E^{red}_{1/2}$ values listed in Table 1 are within 50 mV of the corresponding $E^{\circ}_{XC_6H_4Se^+/XC_6H_4Se^{\bullet}}$ and $E^{\circ}_{XC_6H_4Se^{\bullet}/XC_6H_4Se^-}$ values.

Hammett Plots. In Figures 4 and 5, the values of $E^{ox}_{1/2}$ and $E^{red}_{1/2}$ are plotted against the Hammett substituent coefficient σ^+. We correlate to σ^+ rather than σ or σ^- to be able to compare directly with previous correlations reported for the reduction potentials of substituted phenylthiyl radicals in aprotic solvents[17,39,43,44] and water[45] and phenoxyl radicals in acetonitrile[46] and water.[47] Actually, the correlations with σ are equally good with the following relationships ensuing: $E^{ox}_{1/2} = 0.36\sigma + 0.65$

(43) Bordwell, F. G.; Zhang, X.-M.; Satish, A. V.; Cheng, J.-P. *J. Am. Chem. Soc.* **1994**, *116*, 6605.
(44) Venimadhavan, S.; Amarnath, K.; Harvey, N. G.; Cheng, J.-P.; Arnett, E. M. *J. Am. Chem. Soc.* **1992**, *114*, 221.
(45) Armstrong, D. A.; Sun, Q.; Schuler, R. H. *J. Phys. Chem.* **1996**, *100*, 9892.
(46) Hapiot, P.; Pinson, J.; Yousfi, N. *New J. Chem.* **1992**, *16*, 877.

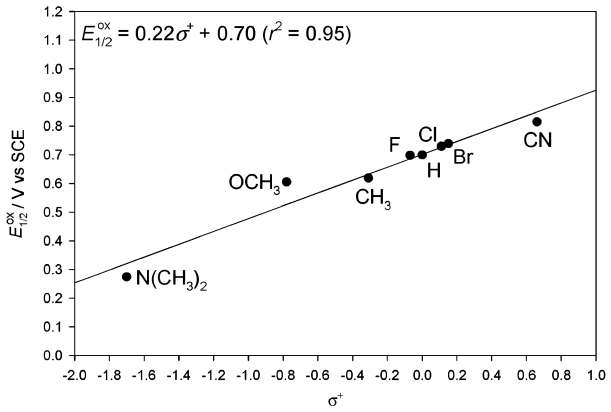

Figure 4. Plot of $E^{ox}_{1/2}$ versus σ^+.

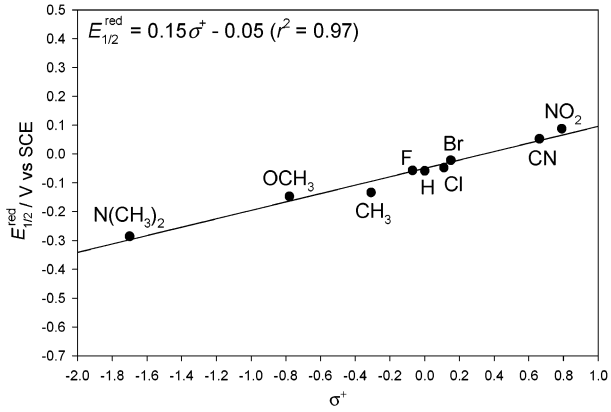

Figure 5. Plot of $E^{red}_{1/2}$ versus σ^+.

Scheme 2

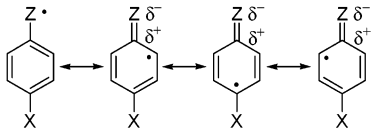

($r^2 = 0.90$) and $E^{red}_{1/2} = 0.23\sigma - 0.09$ ($r^2 = 0.98$). On the other hand, σ^- provides without comparison the poorest correlation (even for $E^{red}_{1/2}$) due to large deviations of the points pertaining to the electron-donating groups, in particular, $N(CH_3)_2$. The reason that σ should be a relatively better correlation parameter in the case of Se as compared to S and O is related to the extent of orbital overlap with the aromatic ring that becomes progressively smaller with size in the order O, S, and Se. In fact, while the bonding between the chalcogen radical center and the aromatic ring has been described essentially as a single bond for phenylthiyl and phenylselanyl radicals, there is double bond character in the case of phenoxyl radicals.[48,49] The latter feature can be attributed to spin delocalization of the odd electron in the radical as illustrated by the resonance structures drawn in Scheme 2 (Z = O, S, or Se).

Note also that the electron-withdrawing ability of the C=Z dipole is much larger for O with an electronegativity of 3.5 than it would be for S and Se with electronegativities of 2.5 and 2.4, respectively. In an earlier study, we investigated the

Table 2. Hammett Slopes, ρ^+, Obtained for the Reduction and Oxidation Potentials of Substituted Phenylselanyl, Phenylthiyl, and Phenoxyl Radicals in Different Solvents

redox couple	ρ^+	solvent	reference
ArSe•ArSe$^-$ [a]	2.5[b]	acetonitrile	this study
ArS•/ArS$^-$ [c]	6.6	sulfolane/3-methylsulfolane (5%)	44
ArS•/ArS$^-$ [c]	6.7	dimethyl sulfoxide	43
ArS•/ArS$^-$ [d]	5.4	acetonitrile	39
ArS•/ArS$^-$ [a]	6.4	acetonitrile	17
ArS•/ArS$^-$ [e]	3.7	water	45
ArO•/ArO$^-$ [d]	10.1	acetonitrile	46
ArO•/ArO$^-$ [e]	7.0	water	47
ArSe$^+$/ArSe• [a]	3.8	acetonitrile	this study
ArS$^+$/ArS• [a]	4.7	acetonitrile	17

[a] Half-wave potentials measured by means of photomodulated voltammetry. [b] The ρ^+ value is 3.4 if $E^{\circ}_{XC_6H_4Se^{\bullet}/XC_6H_4Se^-}$ is used as the correlation parameter rather than $E^{red}_{1/2}$. [c] Irreversible oxidation potentials of the anions measured by means of linear sweep voltammetry. [d] Standard potentials measured by means of fast cyclic voltammetry. [e] Standard potentials measured by means of pulse radiolysis.

substituent effect on the stabilization of phenoxyl radicals due to spin delocalization by analyzing the spin density distribution on the oxygen.[50] It was found that the strongest stabilizing effect was exerted by resonance-donating substituents and that this could explain the observed linear correlation between the O−H bond dissociation energy of phenols and σ^+. This also explains why σ^+ can be the better correlation parameter for $E^{red}_{1/2}$ in the case of phenoxyl radicals but not so in the case of arylthiyl and arylselenyl radicals.

Table 2 presents all relevant slopes ρ^+ obtained from the Hammett plots (based on equilibrium constants) for the substituted phenylselanyl radicals in the present study and for the substituted phenylthiyl and phenoxyl radicals in previous studies.[17,39,43−47] At least a few points are worth noting. First, the values of ρ^+ are positive for both the reduction and the oxidation processes. This agrees with the expectation that electron-donating substituents should make it harder to reduce both the phenylselanyl radicals and the phenylselanylium ions. Another apparent result is the order of ρ^+ values: $\rho^+(XC_6H_4O^{\bullet}) > \rho^+(XC_6H_4S^{\bullet}) > \rho^+(XC_6H_4Se^{\bullet})$ and $\rho^+(XC_6H_4S^+) > \rho^+(XC_6H_4Se^+)$. This illustrates that the substituent effect becomes larger as the π-interaction between the chalcogen center and the aromatic system increases going from Se to S and O. The fact that the slopes $\rho^+(XC_6H_4O^{\bullet})$ and $\rho^+(XC_6H_4S^{\bullet})$ are smaller for aqueous than for aprotic solutions can be attributed to the strong solvation of anions in water in terms of hydrogen bonding. Finally, it should be noted in the case of the arylselanyl radicals that ρ^+ is larger for the oxidation process ($\rho^+ = 3.8$) than for the reduction process ($\rho^+ = 2.5$), which is opposite to the order seen for the S-centered analogues.[17]

Spin States. Before discussing the solvation features of arylselanylium ions, it is important to consider their spin state. At the B3LYP/6-31+G(d) level, the singlet and triplet states of the phenylselanylium ion are very similar in energy. The triplet state is favored over the singlet state by only 3.6 kcal mol^{-1} at 0 K. This can be compared to the singlet−triplet splitting for the phenylsulfenium ion which was computed to be −0.02 kcal mol^{-1} at the same level.[12] At the generally more accurate CBS-QB3 level, the singlet state of the phenylsulfenium ion was found to be favored over the triplet state by 1.53 kcal

(47) Lind, J.; Shen, X.; Eriksen, T. E.; Merényi, G. *J. Am. Chem. Soc.* **1990**, *112*, 479.
(48) Tripathi, G. N. R.; Sun, Q.; Armstrong, D. A.; Chipman, D. M.; Schuler, R. H. *J. Phys. Chem.* **1992**, *96*, 5344.
(49) Kimura, S.; Bill, E.; Bothe, E.; Weyhermüller, T.; Wieghardt, K. *J. Am. Chem. Soc.* **2001**, *123*, 6025.
(50) Brinck, T.; Haeberlein, M.; Jonsson, M. *J. Am. Chem. Soc.* **1997**, *119*, 4239.

Scheme 3

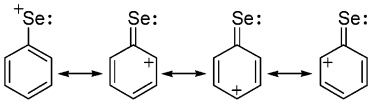

mol^{-1}.[12] We were not able to compute the singlet−triplet splitting of the phenylselanylium ion using the CBS-QB3 method, because this method has not been implemented for compounds containing third row atoms in Gaussian 98. However, if we assume that the error in the B3LYP/6-31+G(d) calculated singlet−triplet splitting is similar for the phenylsulfenium and the phenylselanylium ions, we can estimate the triplet state to be favored over the singlet state by around 2 kcal mol^{-1} in the latter. Without comparison, the energy difference is much more pronounced for alkylselanylium ions. For instance, the singlet−triplet splitting in the methylselanylium ion is 29.7 kcal mol^{-1} according to computations performed at the B3LYP/6-31+G(d) level. Similar results have been obtained in experimental and theoretical studies on alkylsulfenium ions.[51−53] Thus, it is clear that the aromatic ring in the phenylselanylium ion leads to a significant stabilization of the singlet state, which is comparable to that seen in the phenylsulfenium ion. This stabilization can be attributed to charge delocalization due to a favorable resonance interaction between the positive selenium atom and the aromatic ring as illustrated in Scheme 3.

The importance of this resonance interaction can be understood from the computed geometry of the singlet phenylselanylium ion (**1**) depicted in Figure 6. The carbon−carbon bonds in the aromatic ring are strongly alternating in length, and the carbon−selenium bond (1.784 Å) is considerably shorter than a normal single bond (1.94 Å) as predicted from the covalent radii of selenium and carbon.[54] The charge of the selenium atom, which is calculated to be 0.32 au using Mulliken population analysis, is also consistent with the presence of a strong resonance interaction.

The resonance interaction in the triplet state of the phenylselanylium ion (**2**) differs in character from that in the singlet state. In the triplet state, the two lone pair electrons of selenium are divided upon two p-orbitals, and the resonance interaction between the p-orbital perpendicular to the plane of the aromatic ring and the π-system leads to spin delocalization rather than charge delocalization as illustrated in Scheme 4.

A spin density analysis indicates that approximately one-half of an unpaired electron is delocalized over the aromatic system in the triplet state with the highest spin density found over the ortho and para positions. However, the spin delocalization of the triplet state is not expected to lead to as large of a stabilization as the corresponding charge delocalization of the singlet state. The weaker resonance interaction of the triplet state as compared to that of the singlet state is confirmed by less strongly alternating C−C bond lengths and a longer C−Se bond (see Figure 6). There is also a higher charge on selenium in the triplet state (0.44 au) than in the singlet state (0.32 au). As we shall see, the magnitude and sign of the singlet−triplet splitting are affected by substituents, which can be explained by considering the substituent effects on the resonance interactions.

IP and EA. The B3LYP/6-31+G(d) computed values of the singlet and triplet IPs of the phenylselanyl radical, IP(S) and IP(T), are 8.33 and 8.19 eV, respectively. The EA at the same level is 2.25 eV. To our knowledge, no experimental data are available for the phenylselanyl radical. To estimate the reliability of our computations, we can look at the results for the phenylthiyl radical. In this case, IP(S) and EA were computed to 8.43 and 2.27 eV, respectively.[12] The corresponding values obtained at the CBS-QB3 level of theory were 8.48 and 2.41 eV. These results are in relatively good agreement with the experimental determinations of IP = 8.6 ± 0.1 eV and EA = 2.26 ± 0.10 eV.[55] On this basis, we expect the B3LYP/6-31+G(d) computed values for the IPs of arylselanyl radicals to be slightly underestimated but still accurate to within 0.2 eV corresponding to 4.6 kcal mol^{-1} when expressed in free energy units. The computed EAs for arylselanyl radicals are presumably more accurate than the IPs.

In Table 1, the values of IP(S), IP(T), and EA are listed for the different arylselanyl radicals. The electron affinity of the arylselanyl radical is strongly affected by the presence of resonance-withdrawing substituents such as NO_2 and CN. This can be explained by a strong through-resonance interaction between the negatively charged selenium and the substituents at the aromatic ring. Consequently, we also find a good correlation between EA and σ^- following the equation: EA = $0.74\sigma^- + 2.25$, $r^2 = 0.93$. This correlation is better than that between EA and σ: EA = $0.80\sigma + 2.37$, $r^2 = 0.90$. At first it may seem surprising that EA correlates better with σ^- than with σ when the opposite is true for $E^{red}_{1/2}$. However, it should be recalled that $E^{red}_{1/2}$ is a solvent parameter and while solvation diminishes the substituent effect on the stabilization of anions it leaves the stabilization of radicals largely unaffected.

The computed values of IP(S) show that the resonance-donating substituents, $N(CH_3)_2$ and OCH_3, have a strongly stabilizing effect on the arylselanylium ion. There is also a good linear correlation between IP(S) and σ^+ following the equation: IP(S) = $0.83\sigma^+ + 8.28$, $r^2 = 0.97$. This agrees with expectations because there is through-resonance interaction between the positively charged selenium and a resonance-donating substituent. For triplet state cations such an interaction would be predicted to be weaker and indeed the slope obtained for the correlation of IP(T) with σ^+ is smaller: IP(T) = $0.61\sigma^+ + 8.20$, $r^2 = 0.98$ Note that there is a significant substituent effect on the singlet−triplet splitting. While IP(T) is larger than IP(S) by 4−7 kcal mol^{-1} for resonance-donating substituents such as $N(CH_3)_2$ and OCH_3, the opposite is true for the electron-withdrawing NO_2 and CN groups. This trend is not surprising considering that the through-resonance charge delocalization is expected to be larger for the singlet state than for the triplet state. In addition, resonance-withdrawing substituents are known to mediate spin delocalization, which can explain their stabilizing effect on triplet cations.[56−58]

Solvation Energies. To obtain a better understanding of the thermochemistry of selenium-centered anions and cations, we turned our attention toward a calculation of the solvation energies of the two sets of ions on the basis of the electrode potentials measured and the computed ionization potentials and

(51) Rodriquez, C. F.; Hopkinson, A. C. *J. Mol. Struct. (THEOCHEM)* **1987**, *152*, 55.
(52) Pople, J. A.; Curtiss, L. A. *J. Phys. Chem.* **1987**, *91*, 3637.
(53) Curtiss, L. A.; Nobes, R. H.; Pople, J. A.; Radom, L. *J. Chem. Phys.* **1992**, *97*, 6766.
(54) Cotton, F. A.; Wilkinson, G.; Gauss, P. L. *Basic Inorganic Chemistry*, 2nd ed.; John Wiley & Sons: New York, 1987; p 92.
(55) NIST Standard Reference Database No. 69.
(56) Walter, R. I. *J. Am. Chem. Soc.* **1966**, *88*, 1923.
(57) Wayner, D. D. M.; Arnold, D. R. *Can. J. Chem.* **1984**, *62*, 1164.
(58) Jiang, X.-K. *Acc. Chem. Res.* **1997**, *30*, 283.

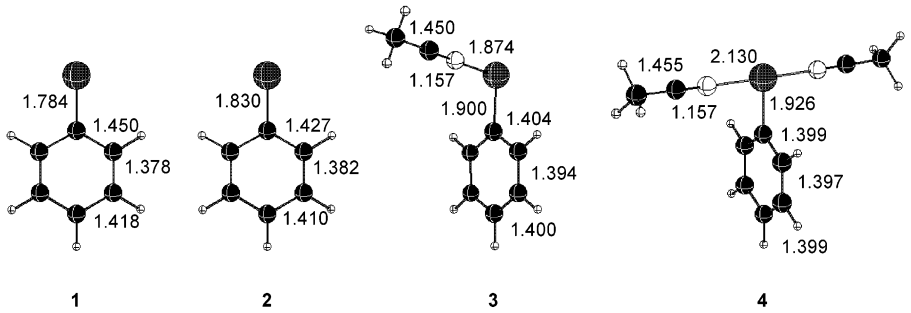

Figure 6. B3LYP/6-31+G(d) optimized structures of the singlet phenylselanylium ion (**1**), the triplet phenylselanylium ion (**2**), the singlet phenylselanylium ion−acetonitrile 1:1 adduct (**3**), and the singlet phenylselanylium ion−acetonitrile 1:2 adduct (**4**).

Scheme 4

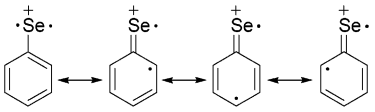

electron affinities (see eqs 3 and 4). In the calculations of $\Delta\Delta G^\circ_{sol}(-\bullet)_{exp}$, we used the values of $E^{red}_{1/2}$ rather than $E^\circ_{XC_6H_4Se^\bullet/XC_6H_4Se^-}$ to be consistent with the corresponding $\Delta\Delta G^\circ_{sol}(+\bullet)_{exp}$ values that were based solely on $E^{ox}_{1/2}$ data. In any case, the effect on $\Delta\Delta G^\circ_{sol}(-\bullet)_{exp}$ is small and within 1−2 kcal mol^{-1} because of the small difference between $E^{red}_{1/2}$ and $E^\circ_{XC_6H_4Se^\bullet/XC_6H_4Se^-}$. With IP data available for both the singlet and the triplet states of the arylselanylium ions, two sets of $\Delta\Delta G^\circ_{sol}(+\bullet)_{exp}$ values might be extracted, in principle, but for reasons that will become clear below, we limited the calculations to include the singlet state only.

The experimentally based solvation data are collected in Table 3 together with the solvation energies $\Delta G^\circ_{sol}(+)_{PCM}$, $\Delta G^\circ_{sol}(-)_{PCM}$, $\Delta G^\circ_{sol}(\bullet)_{PCM}$, $\Delta\Delta G^\circ_{sol}(-\bullet)_{PCM}$, and $\Delta\Delta G^\circ_{sol}(+\bullet)_{PCM}$ computed by the PCM method. For the cations, we have listed values of $\Delta G^\circ_{sol}(S+)_{PCM}$ and $\Delta G^\circ_{sol}(T+)_{PCM}$ for both the singlet and the triplet states. However, in the further calculation of $\Delta\Delta G^\circ_{sol}(+\bullet)_{PCM}$, the singlet state data were the only ones used in agreement with the procedure employed for extracting the corresponding $\Delta\Delta G^\circ_{sol}(+\bullet)_{exp}$ data set. In any case, the difference in the $\Delta G^\circ_{sol}(S+)_{PCM}$ and $\Delta G^\circ_{sol}(T+)_{PCM}$ values is relatively small, although the substituent effect is distinct in the sense that the solvation of the singlet state is more favorable than that of the triplet state for the two most electron-donating groups, OCH_3 and $N(CH_3)_2$, whereas the opposite is true for electron-withdrawing groups such as CN and NO_2. The calculations of $\Delta G^\circ_{sol}(\bullet)_{PCM}$ show that the solvation of the neutral $XC_6H_4Se^\bullet$ species as expected is relatively weak; all values are between 2.8 and 5.6 kcal mol^{-1}. Thus, the substituent effects on $\Delta\Delta G^\circ_{sol}(+\bullet)_{PCM}$ and $\Delta\Delta G^\circ_{sol}(-\bullet)_{PCM}$ are very similar to those on $\Delta G^\circ_{sol}(+)_{PCM}$ and $\Delta G^\circ_{sol}(-)_{PCM}$, respectively.

As for a comparison of the computed and experimental solvation data, there is relatively good agreement between the $\Delta\Delta G^\circ_{sol}(-\bullet)$ values listed in columns 8 and 9, respectively. The most deviating behaviors are seen for the strongly electron-withdrawing and electron-donating groups with $X = N(CH_3)_2$ exhibiting the largest difference of 8 kcal mol^{-1}. This is also illustrated in Figure 7, where the computed solvation energies, $\Delta\Delta G^\circ_{sol}(-\bullet)_{PCM}$, are plotted against the experimental counterparts, $\Delta\Delta G^\circ_{sol}(-\bullet)_{exp}$. The fact that the PCM method works quite well for the anions indicates that the solvation energies are largely determined by the degree of charge delocalization in the system.

The $\Delta\Delta G^\circ_{sol}(-\bullet)_{exp}$ values vary from −58 kcal mol^{-1} in the cases of $X = N(CH_3)_2$ and OCH_3 to −38 kcal mol^{-1} for $X = NO_2$. Accordingly, we also find a linear correlation between $\Delta\Delta G^\circ_{sol}(-\bullet)_{exp}$ and σ^-: $\Delta\Delta G^\circ_{sol}(-\bullet)_{exp} = 12.7\sigma^- - 54.7$, $r^2 = 0.97$. The variation of $\Delta\Delta G^\circ_{sol}(-\bullet)_{exp}$ for the arylselenolates is very similar to that found for the sulfur analogues:[12] $\Delta\Delta G^\circ_{sol}(Se,-\bullet)_{exp} = 1.15\ \Delta\Delta G^\circ_{sol}(S,-\bullet)_{exp} + 13.6$ ($r^2 = 0.98$).

In contrast to the nice consistency in the anion data sets stand the large deviations observed for $\Delta\Delta G^\circ_{sol}(+\bullet)$; the experimental values (column 7) are found to be not only considerably larger in magnitude than the corresponding computed values (column 6) − in many cases by more than 20 kcal mol^{-1} − but also they exhibit a much larger substituent effect as clearly illustrated by the plot of the two data sets in Figure 7.

The decrease in $\Delta\Delta G^\circ_{sol}(+\bullet)_{exp}$ amounts to 31 kcal mol^{-1} as the degree of charge localization in the cations increases going from $X = N(CH_3)_2$ to CN. The following correlation with σ^+ is obtained: $\Delta\Delta G^\circ_{sol}(+\bullet)_{exp} = -13.3\sigma^+ - 65.1$, $r^2 = 0.91$. In general, the absolute values of $\Delta\Delta G^\circ_{sol}(+\bullet)_{exp}$ are larger than those of $\Delta\Delta G^\circ_{sol}(-\bullet)_{exp}$, indicating that the solvation of the cations is stronger than that of the anions. The variation in $\Delta\Delta G^\circ_{sol}(\pm)_{exp}$ listed in the last column of Table 3 is from −31 kcal mol^{-1} for X = CN to 16 kcal mol^{-1} for $X = N(CH_3)_2$. In the case of the phenylselanylium ion with a calculated Mulliken charge of only 0.32 au on the selenium atom, the $\Delta\Delta G^\circ_{sol}(+\bullet)_{exp}$ value of −67 kcal mol^{-1} is even close to the −71 kcal mol^{-1} found for the completely localized and much smaller potassium ion in acetonitrile.[59]

The $\Delta\Delta G^\circ_{sol}(+\bullet)_{exp}$ data set for the arylselenylium ions is almost equal to that for the sulfur analogues, independent of the substituent.[12] Actually, there exists a linear relation with a slope close to unity: $\Delta\Delta G^\circ_{sol}(Se,+\bullet)_{exp} = 0.98\ \Delta\Delta G^\circ_{sol}(S,+\bullet)_{exp} - 2.47$ ($r^2 = 0.95$). In the case of the arylsulfenium ions, we demonstrated that both the large magnitude of $\Delta\Delta G^\circ_{sol}(+\bullet)_{exp}$ as well as the significant substituent effect could be explained on the basis of a supermolecule approach by considering the formation of strong covalent 1:1 adducts between the ions and acetonitrile.[12] Thus, we decided to investigate if similar covalent adducts could be formed for the arylselanylium ions.

The optimized molecular geometry of the singlet phenylselanylium ion−acetonitrile adduct (**3**) is shown in Figure 6. At the B3LYP/6-31+G(d) level, the computed gas-phase binding

(59) Marcus, Y. *Ion Solvation*; John Wiley: Chichester, 1985.

Table 3. Computed Solvation Energies $\Delta G^\circ_{sol}(S+)_{PCM}$, $\Delta G^\circ_{sol}(T+)_{PCM}$, $\Delta G^\circ_{sol}(-)_{PCM}$, $\Delta G^\circ_{sol}(\bullet)_{PCM}$, $\Delta\Delta G^\circ_{sol}(+\bullet)_{PCM}$, and $\Delta\Delta G^\circ_{sol}(-\bullet)_{PCM}$ and Solvation Energies $\Delta\Delta G^\circ_{sol}(+\bullet)_{exp}$, $\Delta\Delta G^\circ_{sol}(-\bullet)_{exp}$, and $\Delta\Delta G^\circ_{sol}(\pm)_{exp}$ Calculated from Experimental Solution Data and Computed Gas-Phase Data[a]

X	$\Delta G^\circ_{sol}(S+)_{PCM}$ [b]	$\Delta G^\circ_{sol}(T+)_{PCM}$ [b]	$\Delta G^\circ_{sol}(-)_{PCM}$ [b]	$\Delta G^\circ_{sol}(\bullet)_{PCM}$ [b]	$\Delta\Delta G^\circ_{sol}(+\bullet)_{PCM}$ [b,c]	$\Delta\Delta G^\circ_{sol}(+\bullet)_{exp}$ [d]	$\Delta\Delta G^\circ_{sol}(-\bullet)_{PCM}$ [b]	$\Delta\Delta G^\circ_{sol}(-\bullet)_{exp}$ [e]	$\Delta\Delta G^\circ_{sol}(\pm)_{exp}$ [f]
$N(CH_3)_2$	−35.1	−32.6	−47.0	3.3	−38.4	−43	−50.3	−58	16
OCH_3	−37.1	−36.3	−51.3	4.2	−41.3	−51	−55.7	−58	7
CH_3	−37.7	−37.9	−50.5	5.6	−43.3	−65	−56.1	−57	−8
F	−42.0	−42.6	−49.3	4.8	−46.8	−67	−54.1	−54	−13
H	−41.5	−41.8	−51.4	4.4	−45.9	−67	−55.9	−56	−11
Cl	−40.2	−41.3	−46.9	4.8	−45.0	−65	−51.7	−51	−13
Br	−39.5	−40.4	−46.7	4.5	−44.0	−63	−51.2	−51	−12
CN	−45.2	−47.9	−43.0	2.8	−48.0	−74	−45.8	−43	−31
NO_2	−46.5	−49.5	−40.2	3.4	−49.9		−43.6	−38	

[a] All values are in kcal mol^{-1}. [b] Calculated at the PCM-B3LYP/6-31+G(d) level. [c] Calculated for the singlet state cation. [d] From eq 3 using the values of IP(S) for the singlet state cation. [e] From eq 4. [f] From eq 5.

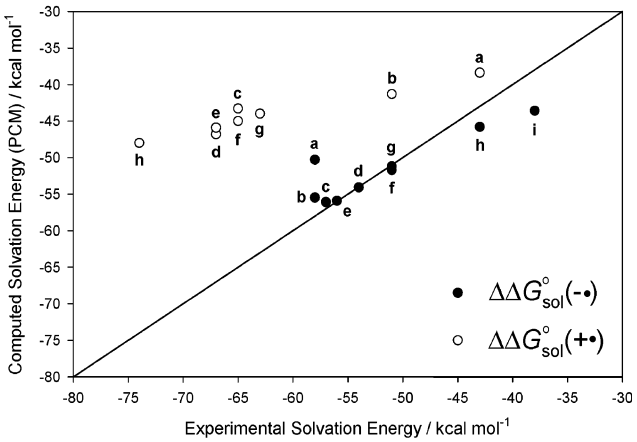

Figure 7. Computed solvation energies obtained at the PCM-B3LYP/6-31+G(d) level versus experimental solvation energies obtained from eqs 3 and 4. The solid line corresponds to a 1:1 relationship between computed and experimental values. Substituents: (**a**) $N(CH_3)_2$; (**b**) OCH_3; (**c**) CH_3; (**d**) F; (**e**) H; (**f**) Cl; (**g**) Br; (**h**) CN; (**i**) NO_2.

enthalpy and free energy of binding are −41.1 and −31.1 kcal mol^{-1}, respectively. The covalent character of the adduct is confirmed by the fact that the Se−N bond length of 1.874 Å is in agreement with the 1.87 Å predicted for a typical Se−N single bond from the covalent radii of selenium and nitrogen.[54] A MP2/6-31+G(d) calculation gave a similar geometry with a Se−N bond length of 1.872 Å, and a slightly more negative binding enthalpy of −44.2 kcal mol^{-1}. The Se−N bond lies in a plane perpendicular to the aromatic ring at an angle of 99°. Furthermore, in contrast to the finding for the isolated singlet phenylselanylium ion (**1**), the aromatic C−C bonds in **3** are almost identical in length. At the same time, the C−Se bond of **3** (1.900 Å) is longer than that of **1** (1.784 Å), and almost as long as a single bond (1.94 Å) as calculated from the covalent radii of carbon and selenium.

These factors together indicate that the resonance interaction between the aromatic π-system and the selenium atom is to a great extent lost in **3**. On the other hand, the geometry of the acetonitrile moiety of **3** is almost identical to that of the free acetonitrile molecule. We can therefore conclude that the Se−N bond can be characterized as a σ-bond arising from the interaction of an empty p-orbital on selenium, which lies perpendicular to the plane of the aromatic ring, and the nitrogen lone-pair orbital of acetonitrile. However, according to the Mulliken population analysis, this is a relatively polar bond, because only 0.47 of an electron has been transferred from the acetonitrile moiety to the phenylselanylium ion. The polar character of the bond is also confirmed by the strong substituent effect on the binding enthalpy; the enthalpy increases from −43.6 to −25.8 kcal mol^{-1} when going from the CN substituent to OCH_3. As we shall see, this can explain the strong substituent effect on $\Delta\Delta G^\circ_{sol}(+\bullet)_{exp}$.

The phenylselanylium ion−acetonitrile adduct is very similar in character and geometry to the previously reported phenylsulfenium ion−acetonitrile adduct.[12] However, the B3LYP/6-31+G(d) calculated binding enthalpy of −41.1 kcal mol^{-1} for the former is considerably smaller than the −28.5 kcal mol^{-1} found for the latter. We can only speculate on the reasons for this difference, but one factor could be that the larger size of the p-orbital on selenium as compared to sulfur leads to a better overlap with the lone pair orbital on acetonitrile. It is also likely that the resonance interaction is weaker in the phenylselanylium ion than in the phenylsulfenium ion, and consequently the loss of the interaction upon forming the bond is energetically less costly in the former.

In our previous study, we noted that the singlet phenylsulfenium ion is not able to bind two acetonitrile molecules covalently.[12] Instead, it was found that the second acetonitrile molecule binds to the phenylsulfenium ion−acetonitrile adduct noncovalently with a binding enthalpy of −9.9 kcal mol^{-1} at the B3LYP/6-31+G(d) level. However, for the singlet phenylselanylium ion, we have been able to locate a favorable structure with two molecules of acetonitrile covalently bonded. This structure is shown as **4** in Figure 6. Calculations at the B3LYP/6-31+G(d) level on the 1:1 adduct **3** show that the binding enthalpy of a second acetonitrile molecule is equal to −21.1 kcal mol^{-1}. Thus, the total binding enthalpy for the two acetonitrile molecules becomes equal to −62.2 kcal mol^{-1}, corresponding to −31.1 kcal mol^{-1} for each of the molecules in the symmetrical **4**. The length of the Se−N bonds in **4** is 2.130 Å, which is considerably larger than the 1.874 Å calculated for the Se−N bond in **3** with the single acetonitrile molecule. We were also able to locate a similar type of complex at the MP2/6-31+G(d) level. The formation of the 1:2 adduct is thus favored as compared to the 1:1 adduct with respect to the binding enthalpy, but as it will be shown below, this does not hold when the free energy of solvation is considered.

For the triplet phenylsulfenium ion, we found that it was unable to form a covalent bond to acetonitrile.[12] Rather, the interaction could be described as a strong van der Waals complex with a S−N bond length of 2.65 Å and a complexation enthalpy of −9.4 kcal mol^{-1}. This behavior of the triplet state was attributed to its lack of an empty p-orbital that could form

Table 4. Computed Solvation Energies $\Delta G^\circ_{sol}(+)_{sup}$ and $\Delta\Delta G^\circ_{sol}(+\bullet)_{sup}$ Using a Combined Supermolecular and PCM Approach for Singlet State Arylselanylium Ion−Acetonitrile 1:1 Adducts and Experimentally Based Solvation Energies $\Delta\Delta G^\circ_{sol}(+\bullet)_{exp}$[a]

X	$\Delta G^\circ_{sol}(+)_{sup}$	$\Delta\Delta G^\circ_{sol}(+\bullet)_{sup}$	$\Delta\Delta G^\circ_{sol}(+\bullet)_{exp}$
OCH_3	−45.5	−49.7	−51
H	−67.5	−71.9	−67
CN	−73.8	−76.6	−74

[a] All values are in kcal mol^{-1}.

a covalent bond with the nitrogen lone-pair orbital. Also, the phenylselanylium ion forms a weaker bond with acetonitrile in the triplet state than in the singlet state, although the difference is less pronounced. With a complexation enthalpy of −19.2 kcal mol^{-1} and a Se−N bond length of 2.52 Å computed at the B3LYP/6-31+G(d) level, the bonding is intermediate between a covalent and a van der Waals bond. Thus, it may be concluded that the singlet phenylselanylium ion should be completely dominating in solution. This result also provides the explanation why we only extracted experimental solvation energies for the singlet ion.

To estimate if the experimental solvation energies of the cations indeed can be explained by the formation of covalent arylselanylium ion−acetonitrile adducts, we decided to calculate $\Delta G^\circ_{sol}(+)$ using the combined supermolecular and PCM approach described in the Theoretical Approach section (see eqs 6 and 7). The $\Delta G^\circ_{sol}(+)_{sup}$ value calculated in the case of the 1:1 adduct **3** is −67.5 kcal mol^{-1}. Thus, the computed solvation energy is lowered by 26 kcal mol^{-1} when compared with the PCM value calculated without an explicit solvent molecule [$\Delta G^\circ_{sol}(+)_{PCM} = -41.5$ kcal mol^{-1}]. A $\Delta\Delta G^\circ_{sol}(+\bullet)_{sup}$ value of −71.9 kcal mol^{-1} is obtained when $\Delta G^\circ_{sol}(\bullet)_{PCM}$ of the phenylselanyl radical is subtracted from the $\Delta G^\circ_{sol}(+)_{sup}$ value, eq 8. This value is in reasonable agreement with $\Delta\Delta G^\circ_{sol}(+\bullet)_{exp} = -67$ kcal mol^{-1}. We also considered the substituent effect on $\Delta G^\circ_{sol}(+)_{sup}$ and $\Delta\Delta G^\circ_{sol}(+\bullet)_{sup}$ by carrying out computations for X = CN and OCH_3. For $\Delta\Delta G^\circ_{sol}(+\bullet)_{sup}$, values of −76.6 and −49.7 kcal mol^{-1} were obtained, respectively, agreeing with the corresponding experimental values of −74 and −51 kcal mol^{-1}. On this basis, we conclude that the large substituent effects on the solvation energies observed experimentally can be explained by the formation of strong 1:1 ion−solvent adducts. In Table 4, all of the above data are collected.

At this point, one should also consider the possibility of having the 1:2 adduct in solution. Calculations of $\Delta\Delta G^\circ_{sol}(+)_{sup2}$ and $\Delta\Delta G^\circ_{sol}(+\bullet)_{sup2}$ in the case of **4** give values of −65.5 and −69.9 kcal mol^{-1}, respectively. These values are slightly larger than those for the 1:1 adduct. Hence, the calculations predict that it is more favorable for the phenylselanylium ion to bind one acetonitrile molecule than two in solution, despite the favorable enthalpy for binding the second molecule as mentioned above. In other words, the latter contribution is overshadowed by the free energy contributions due to loss of translational and rotational entropy and nonspecific solvation. Still, we have to emphasize that the free energy difference is not sufficiently large to make a definite conclusion regarding the coordination number of the phenylselanylium ion.

Conclusions

Reduction and oxidation potentials, $E^{red}_{1/2}$ and $E^{ox}_{1/2}$, of a series of parasubstituted phenylselanyl radicals, $XC_6H_4Se^\bullet$, have been measured using photomodulated voltammetry in acetonitrile. The data obtained for the reduction process were supported by the measurement of the standard potentials, $E^\circ_{XC_6H_4Se^\bullet/XC_6H_4Se^-}$, in linear sweep voltammetry. The absolute mean deviation of the two sets is 50 mV. Both the reduction and the oxidation potentials correlate linearly with the Hammett substituent coefficients σ or σ^+, giving in the latter case slopes ρ^+ of 2.5 and 3.8, respectively. This indicates that the substituent effect is larger on $E^{ox}_{1/2}$ than $E^{red}_{1/2}$. A comparison with literature results obtained for corresponding series of the other chalcogens reveals that $\rho^+(XC_6H_4O^\bullet) > \rho^+(XC_6H_4S^\bullet) > \rho^+(XC_6H_4Se^\bullet)$ and $\rho^+(XC_6H_4S^+) > \rho^+(XC_6H_4Se^+)$, illustrating that the π-interaction becomes progressively smaller as the size of the central atom increases in the order O, S, and Se.

Computed electron affinities and ionization energies have been combined with the experimental reduction and oxidation potentials to obtain solvation energies for the anions and cations. These values have been compared with solvation energies calculated using the PCM approach. For the anions, there is a relatively good agreement both in absolute and in relative terms between the two sets of values. The substituent effect on the solvation energy is found to be determined by the degree of charge separation in the system as manifested by a linear relationship between $\Delta\Delta G^\circ_{sol}(-\bullet)_{exp}$ and the Hammett substituent coefficient σ^-. The numerical values of $\Delta\Delta G^\circ_{sol}(+\bullet)_{exp}$ as well as the substituent effect on $\Delta\Delta G^\circ_{sol}(+\bullet)_{exp}$ are considerably larger than those observed for the corresponding $\Delta\Delta G^\circ_{sol}(-\bullet)_{exp}$ set. The large solvation effects for the cations are not reflected in the computed PCM solvation energies. However, gas-phase calculations show that the singlet arylselanylium ions can form strong Ritter-type adducts with acetonitrile that are similar in character yet stronger than those previously found for the arylsulfenium ions. When this covalent interaction is included in the solvation energy calculations by means of a combined supermolecule and PCM approach, the experimental data are reproduced within a few kcal mol^{-1}. It should be emphasized that all of the above results pertain specifically to the use of acetonitrile as solvent. In a current project, we intend to study the effect of using other solvents as well.

JA0291787